Al-Nahrain Journal for Engineering Sciences

Al-Nahrain J. Eng. Sci. 29(2) 235-246, 2026
Original Article

Leveraging Machine Learning in Modeling and Optimization of Laser Hardening of Aluminum Alloys

Furat I. Hussein[1], Abdulrahman B. Khudhair[2], Hassan T. Mohammed[3] and Suha I. Al-Nassar[4]●.

1,2,3Mechatronics Engineering Department, Al-Khwarizmi College of Engineering, University of Baghdad, Baghdad, 10071 Iraq.
4Department of Communication Engineering, College of Engineering, Diyala University, Iraq.

●*These authors contributed equally to this work*

DOI: https://www.doi.org/10.29194/NJES.29020235

Received: July 30, 2025 **Revised:** Sep. 20, 2025 **Accepted:** Oct. 20, 2025 **Published:** June 20, 2026

Abstract

The current study focuses on utilizing machine learning (ML) models in optimizing and predicting laser-induced surface cold hardening in aluminum alloy 6061-O using a pulsed fiber laser. Three input features were utilized: power density (Pd), frequency (f), and pulse overlap (OV), with surface hardness as the matching aim. A set of ML models, including XGBoost and Adaptive Ensemble, was employed. The dataset was preprocessed for normalization and outlier handling, hyperparameter tuning, and assessment through the grid search and cross-validation, and model performance was evaluated using the coefficient of determination (R^2) and mean square error (MSE) metrics. The Linear regression and Random Forest regression models were excluded due to their weakness in performance, exhibiting noticeable enhancement in performance of the ensemble. After excluding weak models, the results of XGBoost and Adaptive Ensemble models demonstrated great results of R2/MSE of 0.970/0.774 and 0.949/1.319, respectively. The XGBoost model occupied the first order, followed by the Adaptive Ensemble model, in improving the predictive accuracy to around 96% compared to other models.

Keywords: *Machine Learning, XGBoost Model, Adaptive Ensemble Model, Nanosecond Laser, Al 6061-O, Laser Hardening.*

Corresponding author: Provide the corresponding author information and publisher here. E-mail address: furatnejjar@uobaghdad.edu.iq

1. Introduction

Applications of laser-based material processing could utilize machine learning (ML) algorithms to predict potential outcomes and optimize processes by analyzing previous data [1]. Laser hardening is a precise and non-contact surface treatment method widely used to improve metal surface hardness and wear resistance without sacrificing their bulk properties [2]. It involves directing an intense continuous or pulsed laser beam on the surface of the metal being processed, leading to localized heating or melting, followed by rapid cooling due to quenching with the bulk [3]. In aluminum alloys, this thermal cycle may induce intermetallic phases in the processed zone allowing enhanced surface hardness and wear resistance [4]. Laser can be utilized to alloy a thin layer on the surface of aluminum by adding some alloying elements, such as copper, molybdenum, or zirconium, which enhances the surface hardness [5,6]. Another technique utilizes introducing plastic deformation on a thin layer on the surface of aluminum alloy by mechanical means or shocking by laser [7,8]. Nowadays, aluminum alloys are widely involved in the industrial sectors of structural fields, automotive, aerospace, white goods, medical devices, food packaging, electrical, and electronic applications [9-12]. Aluminum alloys are characterized by their lightweight, good weight-to-strength ratio, excellent corrosion resistance, and good electrical and thermal conductivities [13,14]. Unfortunately, their usage in certain applications was limited due to relatively poor strength, hardness, and wear resistance when compared with steel [15]. This drawback is subject to continuous improvements to satisfy the demands of many industry sectors [16]. Laser hardening is a multi-parameter process, variations in these parameters can lead to inconsistent results, necessitating a more systematic and predictive approach to process control. Several highly dependent key parameters, such as laser power, scanning speed, spot size, wavelength, pulse width, frequency of pulses, and overlap percentage, affect the process outcomes [17-19].

ML is an essential aspect of artificial intelligence (AI) that has emerged as a game-changing technology in advanced manufacturing. It enables data mining by analysis of vast datasets to uncover patterns, predict outcomes, and optimize processes [20]. In laser hardening, where multiple parameters interact in complex, nonlinear ways [21], ML techniques can model these relationships swiftly, accurately, and effectively [22]. In the supervised category of ML, regression and classification algorithms are the two essential subcategories [23]. The algorithms of supervised ML are classified according to their applicability in regression, classification, or both [24]. Regression algorithms seek the optimal function that matches the points of the training dataset. Linear regression, multiple linear regression, and polynomial regression are the principal algorithms [25]. Classification algorithms determine the relationship between input and output properties to develop a model that categorizes things into distinct categories based on defined criteria [26]. Logistic regression [27], decision trees [26], support vector machines (SVM) [28], and random forests [29] are utilized in the binary tasks of classification and regression problems. Unsupervised learning techniques, like k-means clustering, further help in identifying inherent groupings in data, aiding in process segmentation and analysis [30].

By integrating ML, manufacturers can reduce reliance on costly and time-intensive trial-and-error experiments, enabling faster process optimization and consistent quality control [31]. The application of ML in laser industrial processes has been the subject of extensive research, showcasing its potential in modelling, classification, and optimization [32]. K. Venkata Rao et al. [33] utilized boring data of a steel alloy in an artificial neural network (ANN) to predict and model surface roughness and vibration during the process. The effect of cutting tool nose radius, speed, and feed rate is investigated. The study demonstrated the ANNs role in the selection of input. Zhang et al. [34] combined two ML algorithms, the grey wolf optimization (GWO) and SVR, to predict the surface roughness and optimize the process parameters of laser-assisted machining process of SiC ceramic. The effect of laser power, turning speed, feed rate, and cutting depths was modeled to predict and optimize the surface roughness. The optimization based on the prediction model showed less than 1.9% between the actual and predicted values of surface roughness, better surface texture, and significant improvement in surface micromorphology. J. Rivera et al. [35] developed an ML model to classify and predict porosity in laser overlap welding of aluminum alloy using a high-speed camera to evaluate the influence of various features on prediction accuracy. D. Buongiorno et al [36] utilized a set of features extracted from a thermal camera during the laser welding process in feeding ML and deep learning (DL) algorithms to a diagnostic framework for weld defect detection. Yunhui Xie et al, [37] adopted reinforcement learning (RL) to manage and monitor a laser machining process of fused silica. Their work was facilitated by the RL algorithm in dynamic control of the laser motion based on real-time feedback, leading to enhanced efficiency. Fengyi Lu et al. [38] utilized deep reinforcement learning in creating a parametric optimization model for multi-pass cutting for the aviation parts capable of giving appropriate decisions that address the diverse cutting situations. The model leverages the predictive power of ML, offering a balanced approach to process modelling and enabling parameter modification to improve energy efficiency within the fluctuating deformation limits of each run.

2. Declaring the Problem and Aim

The industrial community is increasingly adopting laser material processing due to good quality outcomes, accuracy, and ease of setup and processing. However, this route suffers from the difficulties of adjusting the multiple working parameters, which significantly yields inaccuracy and imprecision. Such a problem requires repeating trials to determine the interaction between parameters, resulting in higher costs of technology, maintenance, and operation. The laser hardening process necessitates regulation of process variables such as power, pulse width, frequency, scanning speed, spot size, etc. This request is to know the influence of each parameter on the process outcomes, specifically the hardness level and surfaces free of defects. The current study aims to seek an ML model among various developed and evaluated models that can predict and improve laser surface hardness of aluminum 6061-O using a fiber laser.

3. Experimental

Several square plates, of 7.6 cm side length, of an aluminum grade 6061-O were employed in laser hardening. Table 1 tabulates the elemental composition of the employed alloy. The surface hardness of the raw alloy is 32 HV. Before laser hardening, the aluminum plates were cleaned using acetone and ethanol to remove grease, dust, and surface contamination. After cleaning, one side of each plate was coated with a thin black paint layer (black coat). This coating increases the ability of the surface to absorb laser energy, reduces reflection from the metallic surface, and helps to achieve more uniform heating during the treatment. To treat each square plate with the laser, it was placed in a small container filled with distilled water to a level 3 mm above the upper surface. Figure 1a shows the schematic diagram of the experimental setup, where the laser beam is focused on the upper surface of the plate exactly on the black coat. Based on a CAD model, the pulsed laser beam was selectively scanned and shot 36 small square zones, each having 8 mm side length on the upper surface of the aluminum plate (Figure 1b). These zones were processed with different sets of process parameters.

A Q-switched fiber laser from Wuxi Raycus Fiber Laser Technologies Co., LTD/China, Model WXRFL generates a fundamental wavelength of 1064 ± 4 nm, was used in the process. The laser's average power is 100 W, pulse width 81 ns, and frequency range 10 - 100 kHz. 108 zones on the aluminum plates were processed using three process parameters within specified limits. The laser frequency (f) is in a range of 20 to 25 kHz, the power density (Pd) is within a range of 3.39 to 19.65 GW/cm2, and the percentage of overlap between sequential pulses (OV) for a range from -12 to 78 %.

4. ML Methodology

ML assists in managing multi-variable laser materials processing applications. Integrating experimental data with ML offers a systematic approach to optimizing the process. The following are the essential sequential steps in developing the ML model.

4.1 Definition of the Problem

The current study utilized the findings derived from the experimental results detailed in a previous fundamental study by the authors of this work [39] to develop the ML model for surface hardness. The proposed model passes through several sequential steps starting from the definition of the features and labels of the process.

Three input parameters that influence the surface hardness Pd, f, and OV, were highlighted as input features of the ML model, and the surface hardness was the target. The process of laser hardening of selected zones on aluminum plates produced 108 sets of data derived from experiments.

Table 1. The elemental composition of aluminum 6061-O alloy.

Nominal chemical composition				
Al %	*Mg %*	*Si %*	*Fe %*	*Cr %*
95.8 – 98.6	0.8 – 1.2	0.4 – 0.8	≤ 0.7	0.04 – 0.35
Cu %	*Mn %*	*Ti %*	*Zn %*	*others %*
0.15 – 0.4	≤ 0.15	≤ 0.15	≤ 0.25	≤ 0.15
Experimental chemical composition				
Al %	*Mg %*	*Si %*	*Fe %*	*Cr %*
97.7	0.801	0.571	0.411	0.20
Cu %	*Mn %*	*Ti %*	*Zn %*	*others %*
0.187	0.091	0.062	0.010	0.015

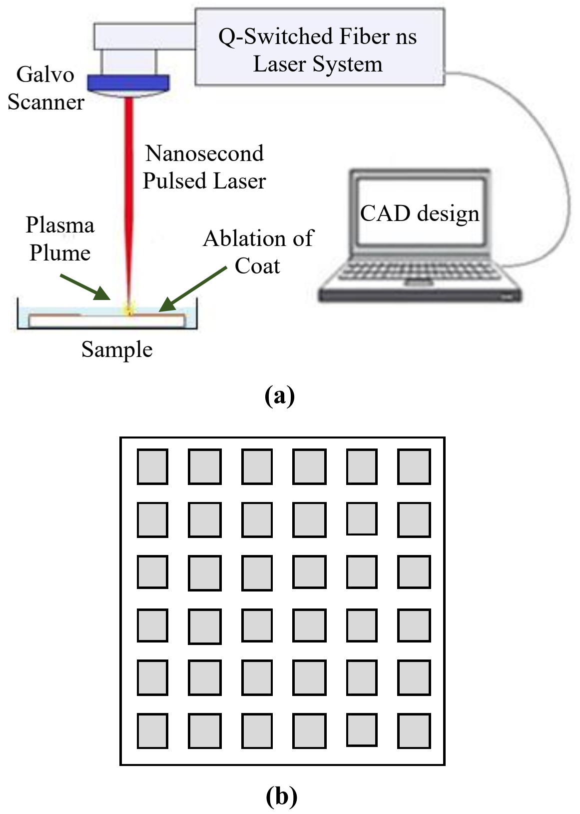

Figure 1. (a) The schematic diagram of the experimental setup, (b) Thirty-six zones on each aluminum single plate processed with the fiber laser.

The Panda's package in Python was used to import the experimental data from an Excel file. Table 2 shows a partial layout for experimental laser hardening data.

4.2 Data Preparation

To improve data quality and enhance the model's performance, reliability, and predictability, the obtained data underwent preprocessing procedures of data cleaning and normalization. All feature values were normalized using Min-Max scaling to ensure consistent input ranges for the ML models, which enhances algorithm performance and convergence. This was done in addition to handling missing and duplicated values, eliminating outliers from the data table, and implementing interpolation. In the second step, the relationship between the features and the target was evaluated to provide a comprehensive view of the effect of each predictor on the target. For this purpose, the correlation matrix was used to display and identify the impact of each feature on the model under development, which could be enhanced by excluding the weak ones after applying additional trials.

The extracted experimental data exhibited non-linear relationships between the input parameters (f, Pd, and OV) and the output (hardness). These relationships were visually observed in the form of curves, where the variation in the output was neither uniform nor linear with the alterations in the input parameters. Figure 2 shows some samples of the effect of manipulating process variables Pd, f, and OV on the surface hardness values.

Table 2. Partial arrangement of the experimental data.

Exp. No.	*f* (kHz)	Pd (GW/cm^2)	*OV* (%)	HD (VHD)
1	20	4.915	75	51.3
2	20	4.915	67.5	49
3	20	4.915	60	48.08
4	20	4.915	52.5	49.15
5	20	4.915	45	51.66
6	20	4.915	37.5	53.88
7	21	4.681		51.32
8	21		34.76	
		16.38	33.34	41.86
101	24	16.38	20.83	41.16
102	24	16.38	8.33	41.54
103	24	16.38	-4.16	42.98
104	25	15.73	60	45
105	25	15.73	48	43.94
106	25	15.73	36	43.36
107	25	15.73	24	43.2
108	25	15.73	12	43.21

4.3 Model Selection, Training, and Evaluation

The non-linear relationship in the experimental datasets challenges analysis, as the linear models are inadequate in predicting the interaction and dependencies between the features and the target. Estimating the input parameters over a large dataset is crucial for accurately predicting in scientific domains [40]. With the abundance of available ML models and algorithms, determining the optimal one for a specific problem is crucial for attaining accurate and meaningful results [41]. To predict and analyze the surface hardness of the alloy, eight ML algorithms were chosen to model the regression of the process. Linear regression, polynomial regression, SVM Regression, Random Forest, Gradient Boosting regression, XGBoost, Decision tree, and adaptive ensemble are utilized for regression problems that involve predicting outcomes [24,42-44].

The dataset was divided into 80% for training and 20% for testing, ensuring an unbiased evaluation of the model's predictive capability. Scikit-learn is a powerful open-source Python library for ML that is beneficial in data preprocessing, model training, evaluation, and optimization [45]. It was utilized for facilities classification, regression, clustering, and dimensionality reduction activities. Employing suitable ML algorithms in regression is essential in making models and optimizing the process. Models are trained via tenfold cross-validation. The comprehensive and quality of trained data is essential for the success of the models in regression and prediction tasks. The Python programming libraries such as NumPy, Pandas, and Scikit-learn have a vital role in building regression models and prediction tasks. The good tuning of the model in the optimization phase avoids the over-fitting or under-fitting of the polynomial degree to ensure robust generalization of new and unseen data benefits in optimization and predicting the surface hardness.

Two techniques, grid search and cross-validation, were employed to offer significant potential for hyperparameter tuning. These parameters are set prior to training and are crucial in shaping model behavior and performance, such as learning rate, number of estimators, and other configuration settings that influence how the model learns, and the assessment of ML models. The grid search systematically evaluated several sets of hyperparameters to discover the optimum model settings, for Random Forest (n_estimators = 50, 100, 200; max_depth = 3, 5, 10) and Gradient Boosting (n_estimators = 50, 100, 200; learning_rate = 0.01, 0.1, 0.2; max_depth = 3, 5). The fold cross-validation technique with 5-fold divides the dataset into sub-folds to evaluate the stability and generalizability on unobserved data by assessing its efficacy across various subsets of the dataset. The optimization techniques are aimed at improving the predictive accuracy, model reliability, and practical applicability. The preceding sub-sections present a comprehensive analysis of the results prior to and subsequent to applying the improvements, evaluating the impact of data preprocessing, feature selection, and hyperparameter tuning on model efficacy.

4.4 Judgement of ML Models

Performance assessment is considered a crucial part of the ML route based on the criteria named performance metrics. The primary criterion is the coefficient of determination (R2) evaluated from the ratio of residuals and the variance of the data. The best fit of the model with the data indicates perfect prediction as R2 approaches one. The R2 is expressed as follows [46]:

$$R^2 = 1 - \frac{\sum_{i=1}^{n}(y_i - y_i^{-})^2}{\sum_{i=1}^{n}(y_i - y^{\wedge})^2} \qquad \text{... (1)}$$

where n is the number of data, yi is the actual value, yi¯ is the predicted value, and y^ is the mean of the actual data.

The mean squared error (MSE) is another key performance metric that quantifies the average difference between actual and predicted values. Model fit and better performance are attained when the residual value approaches its minimum, resulting in the approach of MSE towards zero. MSE is sensitive to outliers since it exaggerates the residuals [47]:

$$MSE = \frac{1}{n}\sum_{i=1}^{n}(y_i - y_i^{-})^2 \qquad \text{... (2)}$$

The accuracy of predicted values in comparison to actual values is assessed by the key performance metrics root mean squared error (RMSE) and mean absolute error (MAE). Like MSE, the values of RMSE and MAE signify enhanced predictive accuracy [48]:

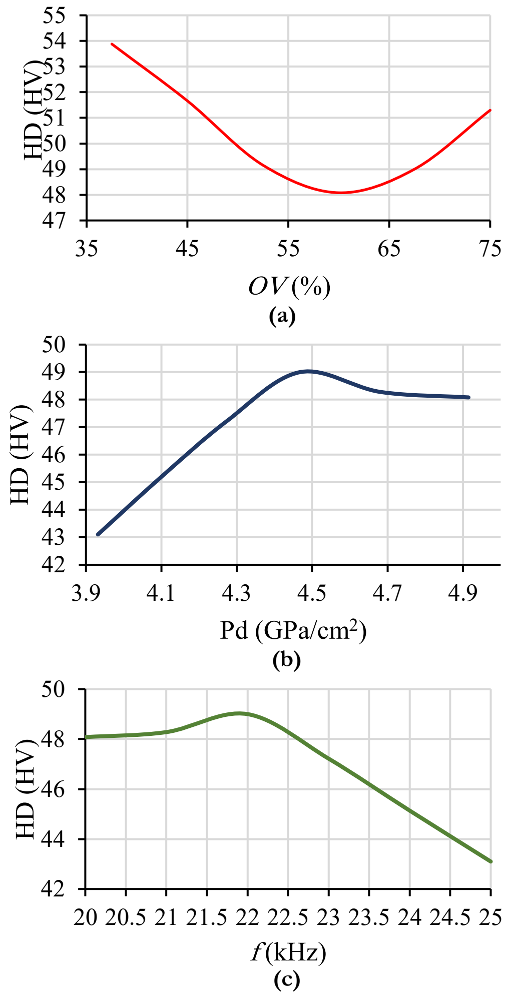

Figure 2. Samples of the influence of surface hardness of aluminum 6061-O by the process variables: (a) OV, (b) Pd, and (c) f.

$$MAE = \frac{1}{n}\sum_{i=1}^{n}|y_i - y_i^{-}| \qquad \text{... (3)}$$

$$RMSE = \sqrt{\frac{1}{n}\sum_{i=1}^{n}(y_i - y_i^{-})^2} \qquad \text{... (4)}$$

Mean Absolute Percentage Error (MAPE) is an estimate that gauges the average absolute deviation between the predicted and actual values within a dataset, providing an evaluation for the errors produced by the model, and can be represented as follows [49]:

$$MAPE = \frac{1}{n}\sum_{i=1}^{n}\frac{|y_i - y_i^{-}|}{y} \qquad \text{... (5)}$$

5. Results and discussions

In the current study, multiple ML algorithms were studied as the main framework in modeling laser hardening of aluminum alloy grade 6061-O using a pulsed fiber laser. ML was utilized in modeling and predicting the relation of Pd, f, and OV with the surface hardness.

5.1 Data Analysis

Visualizing the frequency distribution of the dataset versus input features is beneficial for the model selection and performance (Figure 3). The frequency distribution of features shows a slightly skewed normal distribution for the OV from -20% to 80% indicating wide variability within experiments as shown in Figure 3a. The Pd data in Figure 3b showed three distinct levels of conditions: high, medium, and low constrained due to the three employed laser spot diameters of 0.02 mm, 0.03 mm, and 0.04 mm, respectively. In Figure 3c, the frequency parameter has a unimodal narrow distribution, indicating the employed parameters within a confined range, 20 kHz to 25 kHz, which is imposed by the experimental limitation.

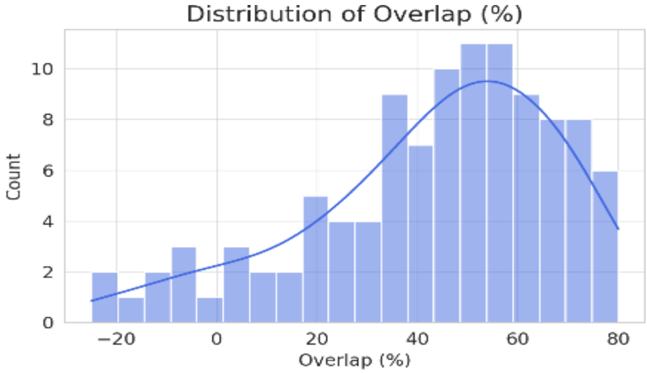

(a)

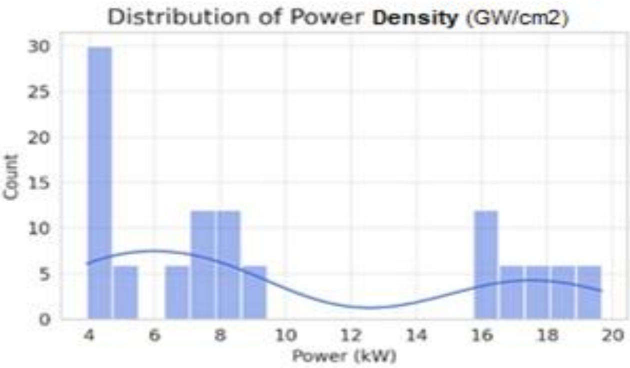

(b)

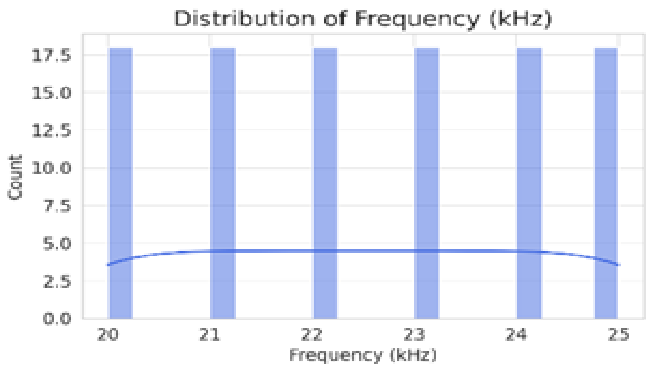

(c)

Figure 3. Frequency distribution of input features: (a) OV, (b) Pd, and (c) f, showing wide variability in OV, three distinct Pd levels, and a narrow, unimodal frequency range.

Figure 4 shows the scatter plot of the relationship between the target and the input feature. The hardness shows an upward trend as the OV became more than 50% as shown in Figure 4a. The hardness values become higher, more unified, and denser at the low levels of Pd, ranging between 4 to 5 GW/cm2, where significant decay in the hardness occurs at the moderate and high values, as Figure 4b. Although the maximum hardness is shown at f of 22 kHz (Figure 4c), there is no significant impact on the hardness, indicating a weak or nonlinear relationship.

The trivial effect of f that disrupts its consideration as an effective factor on the hardness is supported by the negative relation value of -0.099 in the correlation matrix in Figure 4. The Pd and OV show a moderate inverse and direct relationship with the harness of -0.7 and 0.45, respectively. The correlation matrix provides insights into the interrelation of input features, a strong negative correlation of -0.7 between Pd and OV was observed. That reveals that with the higher Pd, the OV should be reduced to avoid the side effect of thermal effects on the metal surface. With both Pd and OV, the f shows a weak negative correlation of -0.13 and a positive correlation of 0.18, respectively.

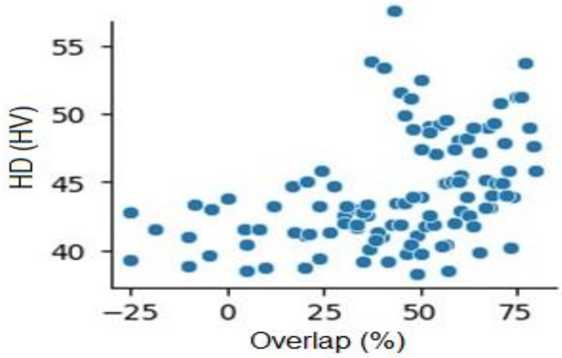

(a)

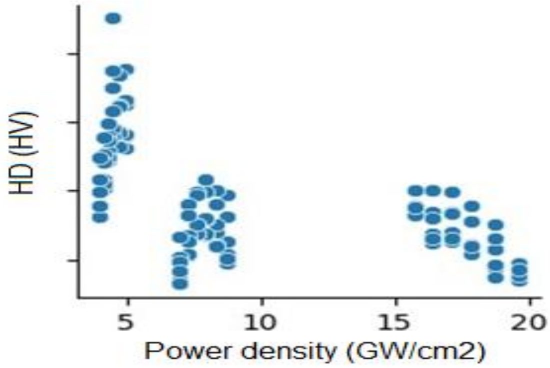

(b)

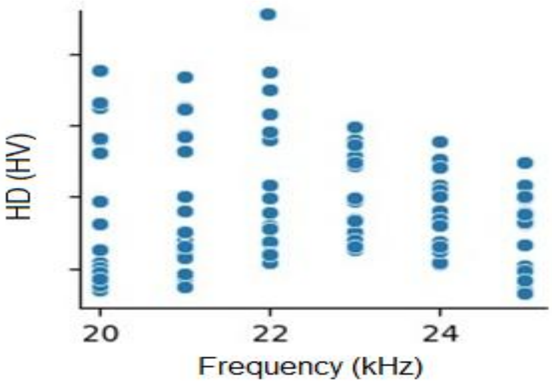

(c)

Figure 4. The relationship between the hardness and input features: (a) OV, (b) Pd, and (c) f. Scatter plots of hardness versus input features, showing an increasing trend with OV > 50%, higher and denser hardness at low Pd.

5.2 Algorithm Testing

The algorithms were tested to evaluate their capabilities in predicting the optimum working parameters to enhance the outcomes of the hardening process. The deployed algorithms were subjected to preprocessing to address errors and outliers in the dataset. Nevertheless, a few of the algorithms showed limitations for various reasons. Table 3 presents the influence of preprocessing on outlier handling for the utilized ML models.

Most models show improvement, in varying degrees, in performance across key metrics. The weakness of the SVM regression model in struggling with regression in the current fed dataset, the instability, and weakness of generalization were present through the value of R2. The average R^2 values obtained from 5-fold cross-validation are presented in the tables for each ML model, both before and after data preprocessing. A significant enhancement is exhibited in the SVM regression model after preprocessing, which showed an increase in R2 from 0.196 to 0.618 and a notable reduction of MSE, MAE, and MAPE. However, the three regression models, linear regression, SVM, and Decision Tree, remain ineffective after preprocessing as indicated by the metric values that signify an inability to capture the complexity of the data.

The Adaptive Ensemble and Polynomial Regression models demonstrated moderate enhancement of performance, displaying R2 of 0.925 and 0.911, respectively, with fewer values of regression error metrics indicating more accurate and robust data fitting. The Gradient Boosting and Random Forest models showed approximately a close to unity R^2 value of 0.947, and lower and approximately equality of metrics errors, indicating stronger predictivity in performance and stability. The preprocessing couldn't enhance the R2 and metrics errors of the XGBoost regression model. Nonetheless, the Gradient Boosting and Random Forest models were surpassed by the XGBoost regression model, showing the highest value of R2 and lower metrics error measures, exhibiting stronger predictive performance and stability.

Table 3. Models of ML before and after preprocessing.

Model	R^2	MSE	RMSE	MAE	MAPE	STD
			Before Preprocessing			
Polynomial Regression	0.839	4.184	2.046	1.532	3.332	5.718
Decision Tree	0.789	5.506	2.346	1.657	3.668	5.728
Random Forest	0.944	1.457	1.207	0.932	2.130	4.726
Gradient Boosting	0.951	1.277	1.130	0.895	2.008	4.968
XGBoost	0.972	0.719	0.848	0.599	1.327	4.933
Linear Regression	0.448	14.380	3.792	3.250	7.266	2.472
SVM Regression	0.196	20.927	4.575	3.840	8.489	1.585
Adaptive Ensemble	0.907	2.410	1.552	1.298	2.954	3.950
			After Preprocessing			
Model	R^2	MSE	RMSE	MAE	MAPE	STD
Polynomial Regression	0.888	2.917	1.708	1.307	2.854	5.123
Decision Tree	0.841	4.142	2.035	1.495	3.364	5.466
Random Forest	0.941	1.534	1.239	0.977	2.202	4.918
Gradient Boosting	0.944	1.446	1.203	0.914	2.054	5.145
XGBoost	0.970	0.774	0.880	0.640	1.438	5.022
Linear Regression	0.443	14.490	3.807	3.267	7.307	2.452
SVM Regression	0.618	9.954	3.155	2.628	5.788	2.450
Adaptive Ensemble	0.932	1.765	1.329	1.064	2.436	4.314

Through boxplots, Figure 5 graphically illustrates the distribution of the input features Pd, f, and OV after outlier handling concerning the target HD. The frequency exhibited the narrowest interquartile range (IQR) around the median, implying a fairly consistent variation in hardness under different conditions of f.

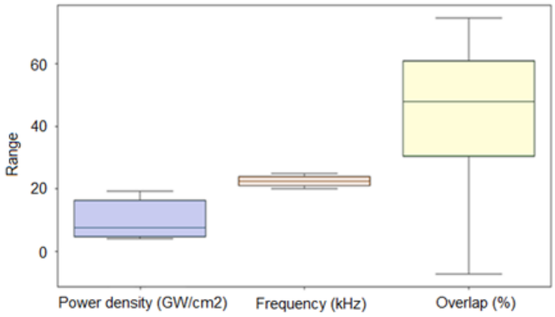

Figure 5. Boxplot of input features after outlier removal, illustrating data distribution and variability for model training.

The OV, in contrast, exhibits a notable expansion in IQR and range, indicating that hardness is affected by a multifaceted connection with this variable. The Pd occupies an intermediate range, indicating moderate variability. The absence of outliers suggests the effectiveness of the preprocessing applied.

The correlation matrix presents the dependency between process variables through the correlation coefficient, which provides the impact and nature of the relationship between variables in the dataset and enhances feature selection [50]. Figure 6 shows the relationships between the input features Pd, f, and OV percentage and the surface hardness of the alloy.

The correlation matrix presents the dependency between process variables through the correlation coefficient, which provides the impact and nature of the relationship between variables in the dataset and enhances feature selection [50]. Figure 6 shows the relationships between the input features Pd, f, and OV percentage and the surface hardness of the alloy after applying laser hardening.

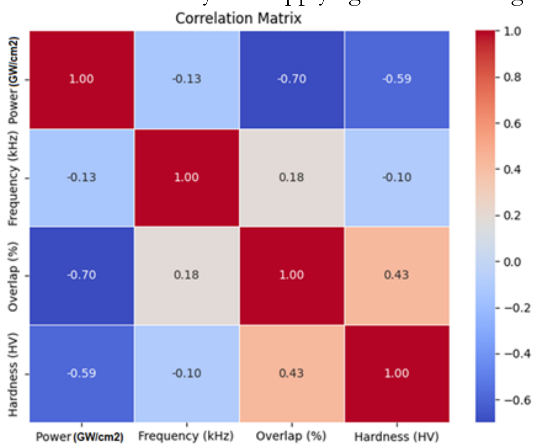

Figure 6. Correlation matrix of input features and target, showing the strength of relationships to guide ML model interpretation.

A moderate and direct relationship of 0.43 between the OV and hardness was observed from the correlation matrix. The moderate relationship of both parameters Pd and OV percentage, with hardness is attributed to their binary effect, irrespective of the nature of directionality. At the lowest sizes of OV, the heating is adequate for ablation of the black coat and building the necessary plasma pressure for cold working. The excessive heating of the surface of the metal occurs when the OV increases, resulting in softening, surface damage, and an increase in hardness due to the heat-treating mechanism and microstructural changes [51]. The correlation coefficient between Pd and hardness of -0.59 indicates a strong and converse relationship. This can be attributed to the alteration of the strain hardening mechanism initiated by the exacerbated plasma pressure, by the excessive heat input leading to material softening or thermal damage [52,53].

The influence of f on surface hardness is extremely weak, as indicated by the negative low correlation coefficient of -0.10, suggesting no direct or negligible relationship between them within the range of experiments used. Nevertheless, the f has an indirect effect on the process due to its contribution to other parameters in heat accumulation per unit area.

The combined interaction between parameters through the inter-parameter relationships between Pd and OV shows a good correlation coefficient of -0.70. This suggests better input feature optimization can yield good performance when higher Pd's are linked with lower OV percentages. On the other hand, the f reveals a weak correlation coefficient with Pd and OV of -0.13 and 0.18, respectively, confirming the negligible influence on hardness under the conditions of the current study. It can be deduced that both Pd and OV are the critical parameters for manipulating the hardness, where an inadequate combination can be deleterious due to thermal effects.

5.3 Model's Ability in Predicting Hardness

Evaluating the lab results with those obtained by employing ML in the test set yields insights into their performance and prediction accuracy. The degree of compliance and the relationship between the actual and the predicted data are presented by the plots in Figure 7. A greater degree of convergence enhances a model's ability to precisely capture the true underlying patterns in the data. The deviation of the point away from the line points to higher disparities between the actual and predicted data. On the other hand, more convergence between the points and the line refers to more accurate predictions and matching the actual data. Evaluation of the ML model performance yielded the following remarks, ordered from the worst to the best in performance accuracy:

1. Linear Regression: Due to its inability to capture nonlinear patterns of datasets, points showed great deviation from the ideal line, suggesting failure of the model in the performance of prediction.
2. SVM Regression: Exhibits a clear separation between the actual and predicted values, as SVM aims to maximize the margin between classes. The model performs well in a few regions of data points only, these points are clustered closely around the ideal line.
3. Decision Tree Regression: Unlike the previous two models, its point distribution showed the same trend of the ideal line, associated with some scattering due to its sensitivity to changes in data.
4. Polynomial Regression: Has common features with the previous Decision Tree model regarding the scattering of points around the ideal line and the accuracy of predictions.
5. Random Forest Regression: More aggregation of data points than in the previous model. The model performance is quite similar to the next model.
6. Gradient Boosting Regression: More concentration of scattered points around the ideal line indicates performance improvement compared with the limitation in the previous models, represented by enhancement of the accuracy of prediction and reduction of errors.
7. Adaptive Ensemble Regression: Although it leverages the strength of predictions from several base models, the points showed limited deviations from the ideal line, which degrade the accuracy of predictions compared with the XGBoost model.
8. XGBoost Regression: The points are concentrated closer to the ideal line, indicating the best predictivity with a higher level of accuracy and effectiveness in capturing the underlying pattern within the data.

5.4 Models Strengths and Limitations

The Taylor diagram, shown in Figure 8, considers multiple measures simultaneously to provide a comprehensive comparison between the observed and predicted models. In addition, this graphical representation highlights an understanding of the strength of each model to replicate patterns and variability, as well as its limitations. It visually combines the standard deviation, correlation factor, and RMSE of models, which are represented by points on the graph relative to the observed model. The distributed points of models close to the reference model are marked as considerably matching the reference model's performance. The following descending-ordered models are the closest models to the reference model: XGBoost, Adaptive Ensemble, Gradient Boosting, Random Forest, Polynomial Regression, and then Decision Tree.

The angle between a model's point and the line of reference point pertains to the gap in the standard deviation and variability relative to the reference model. The XGBoost makes the lower angle, indicating a closer degree of variability with the reference model. On the contrary, the SVM and linear regression models show high variability due to their location at the highest angle among all models. The other models lay on the same radial line, indicating similar spreading and matching in an intermediate level of variability.

The shorter distance between the origin and a model's point suggests its more efficient prediction accuracy. Accordingly, the XGBoost model is the most reliable and robust in hardness predictivity accuracy. The Taylor diagram exhibited that the XGBoost model demonstrated the highest correlation of approximately 0.85, less angle with the reference line indicating less spreading and variability, and minimum RMSE, making it a significant model in performance with accuracy in predictions.

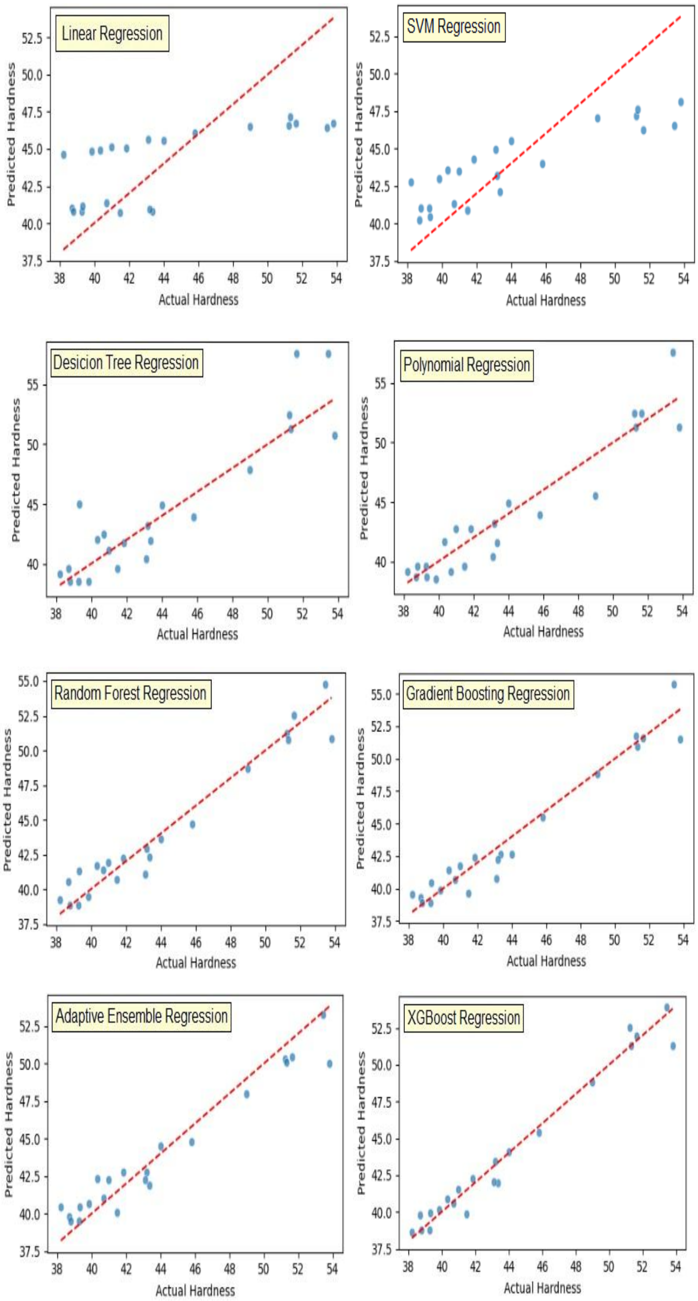

Figure (7): Prediction of hardness by different ML models.

Among the employed eight ML algorithms, the Linear regression, SVM regression models showed underfitting of data, resulting in inaccuracy and failure to hold the non-linear nature of relationships of laser surface hardening. Their presence introduces significant bias to the performance and prediction capability of the ensemble, especially the Adaptive Ensemble model. According to that, the procedures were repeated after excluding these models from the work. The results exhibited a significant enhancement in the Adaptive Ensemble model and a varying degree of improvement in the other model's performance. Figure 9 shows the Taylor graph after eliminating the Linear and SVM regression models. Although the effectiveness of the ensemble as a whole was enhanced by excluding these two weak models, their order of good performance still exists.

The other models, like Gradient Boosting, Random Forest, Decision Tree, and XGBoost demonstrated improvement in demonstrating the variability representation of the experimental hardness values. They showed closer clustering in standard deviation to the reference, more alignment with the observed data, an enhancement in the correlation coefficients, and better values of RMSE. The clustering on the Taylor plot means a reduction in the variance in performance in all models, making the models more robust, consistent, and reliable.

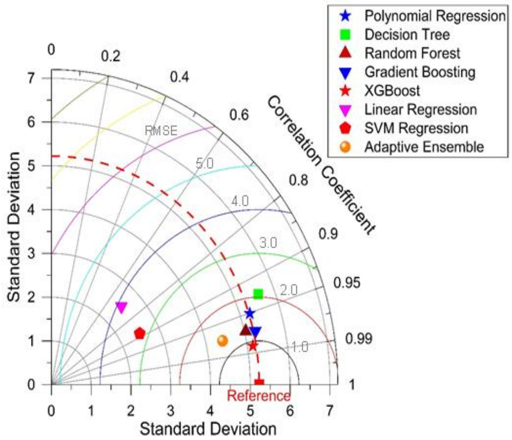

Figure (8): Comparison of utilized ML models through Taylor plot.

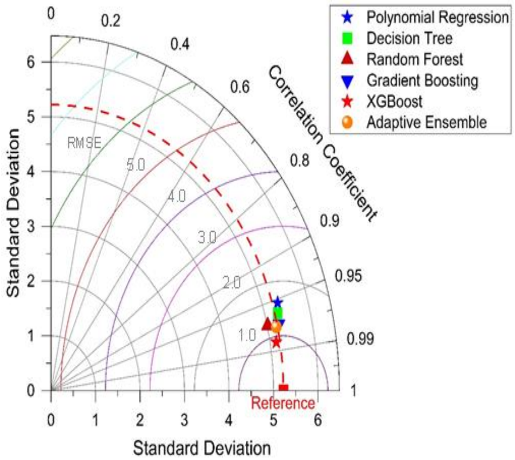

Figure (9): Comparison of utilized ML models after excluding Linear and SVM regression models.

Table (4): Models of ML after eliminating Linear and SVM models, before and after preprocessing.

			Before Preprocessing			
Model	R^2	MSE	RMSE	MAE	MAPE	STD
Polynomial Regression	0.881	3.090	1.758	1.469	3.235	5.085
Decision Tree	0.841	4.130	2.032	1.477	3.232	5.870
Random Forest	0.937	1.635	1.279	1.015	2.266	4.960
Gradient Boosting	0.946	1.398	1.182	0.901	2.024	5.137
XGBoost	0.970	0.774	0.880	0.640	1.438	5.022
Adaptive Ensemble	0.943	1.492	1.221	0.938	2.064	5.257
			After Preprocessing			
Model	R^2	MSE	RMSE	MAE	MAPE	STD
Polynomial Regression	0.896	2.701	1.644	1.275	2.801	5.216
Decision Tree	0.926	1.923	1.387	1.128	2.560	5.165
Random Forest	0.944	1.467	1.211	0.955	2.157	4.897
Gradient Boosting	0.945	1.422	1.192	0.906	2.039	5.142

XGBoost	0.970	0.774	0.880	0.640	1.438	5.022
Adaptive Ensemble	0.949	1.319	1.148	0.897	2.009	5.076

Table 4 tabulates the enhancement in performance metrics without Linear regression and SVM models, before and after preprocessing, and Table 5 presents the percentage of changes in performance metrics after preprocessing. The negative sign in Table 5 refers to a reduction in values after preprocessing and vice versa. The performance metrics show 0% changes before and after preprocessing, revealing a consistent outperform of the XGBoost model among others in both phases. Achieving the highest R^2 of 0.970 and minimum values of error metrics, demonstrating remarkable precision, consistency, and stability in the prediction of this model. The Adaptive Ensemble model benefits from the preprocessing through achieving some enhancement in R^2 value of 0.949 (0.71%) and good reduction of error metrics to be in the second order of strength, and after and close to XGBoost.

The preprocessing significantly improved the performance of the Polynomial Regression, but it kept the last position in the rank of quality among the other five models. A substantial increase in R^2, from 0.841 to 0.926 (1.69%), and a reduction in the error metrics, -12.58% in MSE, observed in the Decision Tree model, which indicates an enhancement in the performance of the model. The Gradient Boosting and Random Forest models kept their good performance before and after preprocessing, represented by their lowest percentage of changes in metrics.

Among the employed eight ML algorithms, the Linear regression, SVM regression models showed underfitting of data, resulting in inaccuracy and failure to hold the non-linear nature of relationships of laser surface hardening. Their presence introduces significant bias to the performance and prediction capability of the ensemble, especially the Adaptive Ensemble model. According to that, the procedures were repeated after excluding these models from the work. The results exhibited a significant enhancement in the Adaptive Ensemble model and a varying degree of improvement in the other model's performance. Figure 9 shows the Taylor graph after eliminating the Linear and SVM regression models. Although the effectiveness of the ensemble as a whole was enhanced by excluding these two weak models, their order of good performance still exists.

The other models, like Gradient Boosting, Random Forest, Decision Tree, and XGBoost demonstrated improvement in demonstrating the variability representation of the experimental hardness values. They showed closer clustering in standard deviation to the reference, more alignment with the observed data, an enhancement in the correlation coefficients, and better values of RMSE. The clustering on the Taylor plot means a reduction in the variance in performance in all models, making the models more robust, consistent, and reliable.

Table 5. The percentage changes in performance metrics after preprocessing.

Model	R^2 (%)	MSE (%)	RMSE (%)	MAE (%)	MAPE (%)
Polynomial Regression	1.69	-12.58	-6.50	-13.18	-13.41
Decision Tree	10.08	-53.45	-31.77	-23.66	-20.79
Random Forest	0.69	-10.24	-5.26	-5.95	-4.79
Gradient Boosting	-0.10	1.71	0.85	0.58	0.76
XGBoost	0.00	0.00	0.00	0.00	0.00
Adaptive Ensemble	0.71	-11.60	-5.98	-4.33	-2.63

5.5 Model Predictions

The importance of each input feature for predicting the surface hardness was computed by applying sensitivity analysis to each parameter. The XGBoost and Adaptive Ensembles models showed close matching in their prediction capabilities. Figure 10 illustrates the sensitivity of XGBoost and Adaptive Ensembles models to the input feature Pd, OV, and f regarding mean absolute SHapley Additive exPlanations (SHAP) values. The latter interprets the contribution of each parameter on the shaping prediction of the model, where the greater values indicate a greater influence on the model's output. The Pd is the most influential parameter with a mean SHAP value of about 2.9, which means changes in this feature have a major impact on the model's prediction. The moderate relevance of OV is indicated by 0.75, followed by the f feature, which showed the least influence in affecting the prediction of an approximate value of about 0.25.

The prediction accuracy across the six models for various input feature ranges demonstrated reliable and consistent predictions. Figure 11 compares the predicted normalized values of the six ML models with the actual values. The clustering of predicted values around feature value ranges suggests harmonizing with the prediction ranges. A strong correlation is noted between all models predictions with actual values, particularly for XGBoost and Adaptive Ensemble, signifying remarkable performance.

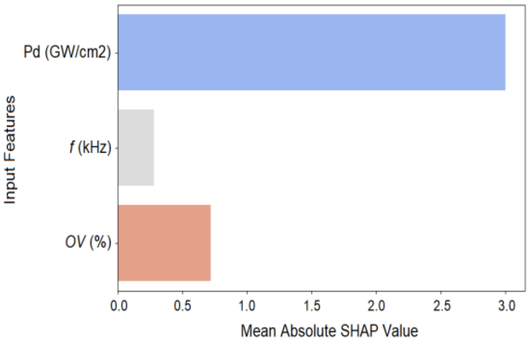

Figure 10. The importance of input features in models' prediction for XGBoost and Adaptive Ensemble models.

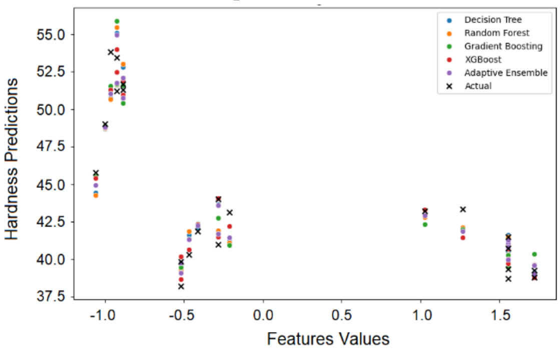

Figure 11. The importance of input features in models' prediction for XGBoost and Adaptive Ensemble models.

6. Conclusions

The study modelled and optimized the surface hardening process through cold working of aluminium alloy employing a nanosecond fiber laser utilizing ML technique. To build a robust, consistent, and reliable model, it is essential to analyze the input features Pd, f, and OV, implement data preprocessing, and handle outliers. The results revealed varying levels of performance of models, showcasing variability in their predictive abilities. The following remarks are concluded from the study:

1. The linear and SVM regression models were ineffective in capturing the nonlinearity of the process and exhibited no or limited improvement in performance after preprocessing. The preprocessing did not alter the changes to the performance metrics of the linear model. Moreover, significantly enhances the performance of SVM by 215.3 % in R2 and 52.43 % in MSE, yet the model is still the least effective among the models and is considered unsuitable in this context.
2. The exclusion of underperforming models, the Linear and SVM regression models, has improved the Adaptive Ensemble model in particular, and overall ensemble performance. This approach resulted in a reduction of bias and enhanced the accuracy of the ensemble.
3. Although the preprocessing did not affect the performance metrics of the XGBoost model by 0% changes, it demonstrated superior performance with high predictive accuracy. The model attained an R2 of 0.970 and an MSE of 0.774, making it the most trustworthy model in predicting surface hardness.
4. After eliminating weak models, the Adaptive Ensemble model ranks second among the powerful models, attaining R2 and MSE values closely approximating those of XGBoost, indicating significant accuracy in prediction.
5. The Gradient Boosting and Random Forest showed good and convergent values of performance metrics and could be qualified as accurate models in prediction.
6. The Polynomial and Decision Tree models exhibited a decline in performance, demonstrating they are not the first suitable choice in predicting the process.
7. The sensitivity analysis of parameters exposed that the Pd has the most significant role in influencing the surface hardness, followed by the OV. The f demonstrated the minimal influence within the examined range of parameters.

The relatively small dataset of 108 and the limited laser frequency range of 20–25 kHz in this study were its limitations. It highlights the potential of ML models—especially XGBoost and Adaptive Ensemble—in predicting laser-induced hardening. The findings can support industrial applications, and future work may explore broader datasets and deeper learning techniques to improve model robustness. Future research may employ processing other types of alloys using another technique, test deep learning models for enhancing prediction accuracy, and study the feasibility of process deployment in an industrial setting.

7. Acknowledgment

The authors gratefully acknowledge the valuable scientific support and constructive input provided by their colleagues at the Department of Mechatronics Engineering - Al-Khwarizmi College of Engineering - University of Baghdad. Their expertise and collaboration contributed meaningfully to the development and refinement of this study.

8. References

[1] S. P. Murzin, "Computer Science Integrations with Laser Processing for Advanced Solutions," Photonics, vol. 11, no. 11, p. 1082, Nov. 2024. https://doi.org/10.3390/photonics11111082

[2] Ł. Łach, "Recent Advances in Laser Surface Hardening: Techniques, Modeling Approaches, and Industrial Applications," Crystals, vol. 14, no. 8, p. 726, Aug. 2024. https://doi.org/10.3390/cryst14080726

[3] E. Anusha, A. Kumar, and S. M. Shariff, "A novel method of laser surface hardening treatment inducing different thermal processing condition for thin sectioned 100Cr6 steel," Opt. Laser Technol., vol. 125, p. 106061, May 2020. https://doi.org/10.1016/j.optlastec.2020.106061

[4] W. Pakieła, T. Tanski, Z. Brytan, G. Chladek, and K. Pakieła, "Impact of laser surface treatment on microstructure, wear resistance and hardness of AlMg5 aluminum alloy," Appl. Phys. A, vol. 126, no. 3, p. 231, Mar. 2020. https://doi.org/10.1007/s00339-020-3350-x

[5] M. Karamimoghadam, M. Rezayat, M. Moradi, A. Mateo, and G. Casalino, "Laser surface transformation hardening for automotive metals: Recent progress," Metals, vol. 14, no. 3, p. 339, Mar. 2024. https://doi.org/10.3390/met14030339

[6] A. P. I. Popoola, O. S. Fatoba, H. W. Nkosi, and V. S. Aigbodion, "Surface hardening of aluminium by laser alloying with molybdenum and zirconium powder," Int. J. Electrochem. Sci., vol. 11, no. 1, pp. 126-139, 2016. https://doi.org/10.1016/S1452-3981(23)15831-7

[7] J. Sawangpan, S. Panich, T. Jantarasricha, and A. Khantachawana, "Investigation of surface hardness and roughness on formability of aluminum alloy sheet AA2024 T3 subjected to shot peening by silica shots," J. Met. Mater. Miner., vol. 33, no. 1, pp. 56-64, Mar. 2023. https://doi.org/10.55713/jmmm.v33i1.1594

[8] J. Kaufman, M. Bohm, J. Brajer, and S. Zulic, "Laser shock peening of aluminium alloys to enhance surface properties," MM Sci. J., vol. 2019, no. 05, pp. 3638-3642, Dec. 2019. https://doi.org/10.17973/MMSJ.2019_12_2019114

[9] N. Hung and M. Marion, "Improved formability of aluminum alloys using laser induced hardening of tailored heat treated blanks," Phys. Procedia, vol. 39, pp. 318-326, 2012. https://doi.org/10.1016/j.phpro.2012.10.044

[10] S. Li, J. Zhang, Y. Chen, X. Wang, L. Zhao, and M. Zhou, "Development and applications of aluminum alloys for aerospace industry," J. Mater. Res. Technol., vol. 27, pp. 944-983, Nov. 2023. https://doi.org/10.1016/j.jmrt.2023.09.274

[11] D. Varshney and K. Kumar, "Application and use of different aluminium alloys with respect to workability, strength and welding parameter optimization," Ain Shams Eng. J., vol. 12, no. 1, pp. 1143-1152, Mar. 2021. https://doi.org/10.1016/j.asej.2020.05.013

[12] D. Ashkenazi, "How aluminum changed the world: A metallurgical revolution through technological and cultural perspectives," Technol. Forecast. Soc. Change, vol. 143, pp. 101-113, Jun. 2019. https://doi.org/10.1016/j.techfore.2019.03.011

[13] A. R. Alhamaoy, G. S. Sadiq, F. I. Hussein, and S. N. Ali, "Cyclic fatigue behavior for 6061 T6 Al alloy shafts processed by laser shock peening," Mater. Sci. Forum, vol. 1002, pp. 21-32, 2020. https://doi.org/10.4028/www.scientific.net/MSF.1002.21

[14] M. Dada and P. Popoola, "Recent advances in joining technologies of aluminum alloys: A review," Discov. Mater., vol. 4, no. 1, p. 86, Dec. 2024. https://doi.org/10.1007/s43939-024-00155-w

[15] A. Gujba and M. Medraj, "Laser peening process and its impact on materials properties in comparison with shot peening and ultrasonic impact peening," Materials, vol. 7, no. 12, pp. 7925-7974, Dec. 2014. https://doi.org/10.3390/ma7127925

[16] C. R. Song, Y. Zhang, L. Chen, M. Liu, H. Zhao, and F. Wang, "Recent progress of Al-Mg alloys: Forming and preparation process, microstructure manipulation and application," J. Mater. Res. Technol., vol. 31, pp. 3255-3286, Jul. 2024. https://doi.org/10.1016/j.jmrt.2024.07.051

[17] M. Moradi, H. Arabi, and M. Shamsborhan, "Multi objective optimization of high power diode laser surface hardening of AISI 410 using RSM and desirability approach," Optik, vol. 202, p. 163619, Feb. 2020. https://doi.org/10.1016/j.ijleo.2019.163619

[18] A. M. El Batahgy, R. A. Ramadan, and A. R. Moussa, "Laser surface hardening of tool steels-Experimental and numerical analysis," J. Surf. Eng. Mater. Adv. Technol., vol. 3, no. 2, pp. 146-153, 2013. https://doi.org/10.4236/jsemat.2013.32019

[19] A. J. Haider, T. Alawsi, M. J. Haider, B. A. Taha, and H. A. Marhoon, "Comprehensive review on pulsed laser deposition technique for nanostructure production: Trends and challenges," Opt. Quantum Electron., vol. 54, no. 8, p. 488, Aug. 2022. https://doi.org/10.1007/s11082-022-03786-6

[20] S. Xiao, J. Li, Z. Wang, Y. Chen, and S. Tofighi, "Advancing additive manufacturing through machine learning techniques: A state of the art review," Future Internet, vol. 16, no. 11, p. 419, Nov. 2024. https://doi.org/10.3390/fi16110419

[21] A. G. Jerniti, A. El Ouafi, and N. Barka, "Predictive modeling based on regression and artificial neural networks for laser transformation hardening of cylindrical steel workpieces," J. Surf. Eng. Mater. Adv. Technol., vol. 6, no. 4, pp. 149-163, 2016. https://doi.org/10.4236/jsemat.2016.64014

[22] C. L. Mambuscay, C. Ortega Portilla, J. F. Piamba, and M. G. Forero, "Predictive modeling of Vickers hardness using machine learning on D2 steel with various treatments," Materials, vol. 17, no. 10, p. 2235, May 2024. https://doi.org/10.3390/ma17102235

[23] R. Nath Mohalder, M. Alam Hossain, and N. Hossain, "Classifying supervised machine learning and comparing algorithm performance," Int. J. Adv. Res., vol. 12, no. 1, pp. 422-438, Jan. 2024. https://doi.org/10.21474/IJAR01/18138

[24] I. H. Sarker, "Machine learning: Algorithms, real world applications and research directions," SN Comput. Sci., vol. 2, no. 3, p. 160, May 2021. https://doi.org/10.1007/s42979-021-00592-x

[25] M. M. Taye, "Understanding machine learning with deep learning: Architectures, workflow, applications and future directions," Computers, vol. 12, no. 5, p. 91, Apr. 2023. https://doi.org/10.3390/computers12050091

[26] B. Charbuty and A. Abdulazeez, "Classification based on decision tree algorithm for machine learning," J. Appl. Sci. Technol. Trends, vol. 2, no. 1, pp. 20-28, Mar. 2021. https://doi.org/10.38094/jastt20165

[27] M. Maalouf, "Logistic regression in data analysis: An overview," Int. J. Data Anal. Tech. Strateg., vol. 3, no. 3, pp. 281-299, 2011. https://doi.org/10.1504/IJDATS.2011.041335

[28] R. Guido, S. Ferrisi, D. Lofaro, and D. Conforti, "Advancements of support vector machine models in healthcare applications: A review," Information, vol. 15, no. 4, p. 235, Apr. 2024. https://doi.org/10.3390/info15040235

[29] Z. Jin, J. Shang, Q. Zhu, C. Ling, W. Xie, and B. Qiang, "RFRSF: Employee turnover prediction using random forests and survival analysis," Lect. Notes Comput. Sci., vol. 12343, pp. 503-515, 2020. https://doi.org/10.1007/978-3-030-62008-0_35

[30] S. Naeem, A. Ali, S. Anam, and M. M. Ahmed, "Unsupervised machine learning algorithms: Comprehensive review," Int. J. Comput. Digit. Syst., vol. 13, no. 1, pp. 911-921, Apr. 2023. https://doi.org/10.12785/ijcds/130172

[31] "Advanced manufacturing with machine learning: Enhancing predictive maintenance, quality control, and process optimization," Al Rafidain J. Eng. Sci., vol. 2, no. 2, pp. 280-300, Sep. 2024. https://doi.org/10.61268/6mvqve13

[32] A. N. Bakhtiyari, Z. Wang, L. Wang, and H. Zheng, "Applications of artificial intelligence in modeling and optimization of laser beam machining: A review," Opt. Laser Technol., vol. 135, p. 106721, Mar. 2021. https://doi.org/10.1016/j.optlastec.2020.106721

[33] K. V. Rao, K. P. Vidhu, T. A. Kumar, N. N. Rao, P. B. G. S. N. Murthy, and M. Balaji, "ANN approach to investigate surface roughness and vibration in boring of AISI 1040 steels," Int. J. Adv. Manuf. Technol., vol. 83, no. 5-8, pp. 919-927, Mar. 2016. https://doi.org/10.1007/s00170-015-7621-1

[34] C. Cao, Y. Zhang, L. Chen, M. Liu, H. Zhao, and F. Wang, "Prediction and optimization of surface roughness for laser assisted machining of SiC ceramics using improved SVR," Micromachines, vol. 13, no. 9, p. 1448, Sep. 2022. https://doi.org/10.3390/mi13091448

[35] J. S. Rivera, M. O. Gagné, S. Tu, N. Barka, F. Nadeau, and A. El Ouafi, "Quality classification model for porosity prediction in laser welding of aluminum alloys," J. Laser Appl., vol. 35, no. 2, May 2023. https://doi.org/10.2351/7.0000769

[36] D. Buongiorno, F. Rossi, L. Bianchi, M. Conti, A. Romano, and S. Greco, "Inline defective laser weld identification using thermal image sequences and machine learning," Appl. Sci., vol. 12, no. 13, p. 6455, Jun. 2022. https://doi.org/10.3390/app12136455

[37] Y. Xie, M. Praeger, J. A. Grant Jacob, R. W. Eason, and B. Mills, "Motion control for laser machining via reinforcement learning," Opt. Express, vol. 30, no. 12, p. 20963, Jun. 2022. https://doi.org/10.1364/OE.454793

[38] F. Lu, G. Zhou, C. Zhang, Y. Liu, F. Chang, and Z. Xiao, "Energy efficient multi pass cutting parameter optimization for aviation parts using deep reinforcement learning," Robot. Comput. Integr. Manuf., vol. 81, p. 102488, Jun. 2023. https://doi.org/10.1016/j.rcim.2022.102488

[39] F. I. Hussein, S. Al Sumaidae, A. Alhamaoy, K. N. Salloomi, and M. A. Obeidi, "Selective laser hardening of aluminium AA6061 O alloy with nanosecond laser pulses," Diyala J. Eng. Sci., pp. 120-135, Mar. 2025. https://doi.org/10.24237/djes.2025.18107

[40] K. Kumar, "Machine learning in parameter estimation of nonlinear systems," pp. 1-22, 2023.

[41] E. Barbierato and A. Gatti, "Challenges of machine learning: A critical review," Electronics, vol. 13, no. 2, p. 416, Jan. 2024. https://doi.org/10.3390/electronics13020416

[42] D. A. Gzar, A. M. Mahmood, and M. K. Abbas, "Comparative study of regression machine learning algorithms: Accuracy vs. computational complexity," Math. Model. Eng. Probl., vol. 9, no. 5, pp. 1217-1224, Dec. 2022. https://doi.org/10.18280/mmep.090508

[43] H. Mao, J. Meng, F. Ji, Q. Zhang, and H. Fang, "Comparison of ML regression algorithms for cotton leaf area index retrieval using Sentinel 2 bands," Appl. Sci., vol. 9, no. 7, p. 1459, Apr. 2019. https://doi.org/10.3390/app9071459

[44] J. Mendes Moreira, C. Soares, A. M. Jorge, and J. F. De Sousa, "Ensemble approaches for regression: A survey," ACM Comput. Surv., vol. 45, no. 1, 2012. https://doi.org/10.1145/2379776.2379786

[45] S. Raschka, Y. Liu, and V. Mirjalili, Machine Learning with PyTorch and Scikit Learn, 2022.

[46] R. K. Tipu, V. Batra, Suman, V. R. Panchal, and K. S. Pandya, "Predictive modelling of surface chloride concentration in marine concrete structures," Asian J. Civ. Eng., vol. 25, no. 2, pp. 1443-1465, Feb. 2024. https://doi.org/10.1007/s42107-023-00854-4

[47] T. O. Hodson, T. M. Over, and S. S. Foks, "Mean squared error, deconstructed," J. Adv. Model. Earth Syst., vol. 13, no. 12, 2021. https://doi.org/10.1029/2021MS002681

[48] B. V. Varma, E. V. Prasad, and S. Singha, "Predicting compressive strength of concrete using supervised ML techniques," Asian J. Civ. Eng., vol. 24, no. 7, pp. 2549-2560, Nov. 2023. https://doi.org/10.1007/s42107-023-00662-w

[49] A. Jierula, S. Wang, T. M. Oh, and P. Wang, "Accuracy metrics for predicting damage locations in deep piles using ANN and acoustic emission data," Appl. Sci., vol. 11, no. 5, p. 2314, Mar. 2021. https://doi.org/10.3390/app11052314

[50] A. F. AlShammari, "Feature selection using correlation matrix in Python," Int. J. Comput. Appl., vol. 186, no. 58, pp. 29-34, Dec. 2024. https://doi.org/10.5120/ijca2024924341

[51] F. I. Hussein, E. Akman, K. N. Salloomi, K. I. Hajim, and A. Demir, "Evaluation of PMMA joining to stainless steel 304 using pulsed Nd:YAG laser," Opt. Laser Technol., vol. 49, pp. 143-152, Jul. 2013. https://doi.org/10.1016/j.optlastec.2012.12.028

[52] F. I. Hussein, K. N. Salloomi, E. Akman, K. I. Hajim, and A. Demir, "Finite element thermal analysis for PMMA/stainless steel 304 laser direct joining," Opt. Laser Technol., vol. 87, pp. 64-71, Jan. 2017. https://doi.org/10.1016/j.optlastec.2016.07.017

[53] M. E. Palmieri and L. Tricarico, "Laser heat treatment strategies for local softening of age hardening aluminum alloy sheets," J. Mater. Eng. Perform., vol. 33, no. 18, pp. 9612-9625, Sep. 2024. https://doi.org/10.1007/s11665-024-09522-3